On the Reliability of Safety Message Broadcast in Urban Vehicular Ad hoc Networks

Saeed Bastani[†,‡] Bjorn Landfeldt[†] Lavy Libman[†,‡]
[†]School of Information Technologies, University of Sydney, NSW 2006, Australia
[‡]Networks research group, NICTA, 13 Garden St., NSW 1430, Australia
sbastani@it.usyd.edu.au, bjorn.landfeldt@sydney.edu.au, lavy.libman@sydney.edu.au

ABSTRACT
Road safety is one of the most important emerging applications envisioned for Vehicular Ad hoc Networks (VANETs). Generally, such applications involve the broadcast of safety messages, consisting of beacons transmitting vehicles' state (e.g. position and velocity) with a regular period, as well as emergency messages warning about unexpected critical events. From the perspective of safety, the application performance depends foremost on two metrics: for the event-driven warning messages, the probability of message reception; and for periodic messages, the variability of the inter-reception time (IRT), which ultimately determines the freshness of the information received by the driver. In this paper, we develop an analytical model to compute the above metrics in an urban traffic scenario. Focusing on a road segment linked to a signalized junction as a basic building block of urban traffic systems, we apply a novel road traffic density model to investigate the dynamics of the reliability metrics and characterize the region(s) on the road segment according to the achieved safety level. Our numerical study shows that in broadcast mode, the hidden terminal effect is the driving factor determining the reliability of transmissions. Furthermore, the impact of hidden terminals has the greatest effect in road sections where vehicles have high velocity, leading to the poorest performance in regions where reliable reception is needed the most in order to minimize the risk of accidents.

Categories and Subject Descriptors
C.2.1 [**Network Architecture and Design**]: Wireless Communication

General Terms
Performance, Theory

Keywords
Vehicular Traffic Density; Vehicular Ad hoc Networks; Safety Applications;

1. INTRODUCTION
Vehicular Ad hoc Networks (VANETs) have recently attracted significant research and development efforts from different players including academia, standards bodies, and industry, leading to the emergence of DSRC/WAVE [1][2] as a reference standard, numerous dissemination/forwarding schemes [3], and several active projects [4]. Inter-vehicle communications open the door for a plethora of applications and services to provide safety and comfort through wireless vehicle-to-vehicle communications. Comfort applications are expected to improve the passengers' travel experience and optimize traffic efficiency, while the safety applications aim at minimizing accident levels. Safety applications can be categorized further according to their use of either periodic or event-driven messages. The first category has an informative nature, as messages are disseminated among vehicles regularly to inform drivers about local parameters such as speed and position. Event-driven messages, on the other hand, are broadcast by vehicles whenever they experience or detect a hazard or otherwise notable event. Single hop broadcast is the fundamental mechanism of periodic safety message dissemination in VANETs. In case of event-driven warning messages, even though broadcast over multiple hops may be used, the ultimate message dissemination performance depends foremost on the performance of each single hop broadcast involved.

The reliability of message broadcasts in a safety application is key to its credibility and ultimate acceptance by the drivers as the end users. Depending on the type and purpose of a safety message, a subset of parameters describes the reliability of the safety application. For event-driven messages, the reliability of the safety application is determined by the successful packet reception probability and geographical coverage of message dissemination. On the other hand, in case of periodic messages, inter-reception time (IRT) of messages is a good candidate metric for describing the application reliability. The IRT metric incorporates the variability of message reception time and packet reception probability into a single parameter. Intuitively, from a recipient vehicle perspective, a high probability of message reception from neighbor vehicles leads to high overall awareness by the recipient about its neighborhood. Furthermore, a high frequency message reception enhances the information freshness a recipient maintains at any time instance, and, in turn, promotes timely reaction to undesired events as they occur. Correspondingly, from a sender point of view, the higher the chance that the neighbor vehicles receive its message successfully and timely, the better the achieved safety level will be.

The key factor impacting the reliability metrics mentioned above is traffic density. In static wireless networks, due to the deterministic distribution of nodes throughout the network area, it is straightforward to characterize the traffic behavior and thus reliability metrics. On the other hand, in vehicular ad hoc networks (as in mobile ad hoc networks in general), characterizing reliability involves taking into account dynamic topology changes due to vehicles' mobility, which in turn is affected by microscopic and macroscopic traffic parameters [5][6][7]. These parameters include, but are not limited to, traffic regulations on junctions and road segments, driver behavior, traffic flow, road capacity, *etc*. In vehicular networks, the analysis of the reliability of a safety application is even more complicated than in other mobile ad hoc networks, due to the impact of unexpected drivers' behavior and

[‡]NICTA is funded by the Australian Government as represented by the Department of Broadband, Communications and the Digital Economy and the Australian Research Council through the ICT Centre of Excellence program.

MSWiM'11, Oct 31–Nov 4, 2011, Miami Beach, FL, USA.

variable traffic flow on vehicles' mobility [7]. Moreover, it is also expected that the reliability varies significantly between highway and urban VANET scenarios. This is partly due to the fact that traffic density is homogeneous under free and stable traffic flow regimes, which dominate highways, whereas a mixture of different traffic densities can be observed simultaneously in an urban scenario as simple as a road segment linked to a signalized junction. Moreover, an urban traffic network must be seen as a 2-dimensional network, compared to a 1-dimensional highway network. This makes the dynamics of traffic density more complicated in urban scenarios, resulting in more complex reliability behavior, especially near junctions.

In line with the above, we are motivated to apply a traffic density model of a simple urban traffic scenario comprising a signalized junction and road segments linked to that junction to analytically describe the spatial-temporal behavior of safety messages' reliability throughout an urban road segment. In the proposed analytical model, the probability of successful message transmission associated with both periodic and warning messages contending for a shared channel are calculated. Additionally, we determine the distribution function corresponding to the IRT of beacon messages. In this work we are not interested in the per-message channel access delay, as this is in the order of a few milliseconds and thus not a key factor impacting the requirements of a safety application [8]. Transmission failures, on the other hand, are of high importance, since in the case of periodic messages a single transmission failure causes the reception time to exceed a beacon interval as large as 100ms [8].

The remainder of this paper is organized as follows. Section 2 provides an overview of related work. In section 3, we develop a general Markovian analytical framework to characterize the reliability metrics of safety message broadcast, and apply it with an urban traffic density model in section 4. A numerical evaluation of the model is presented in section 5, and finally, section 6 concludes the paper.

2. Related Work

Safety message broadcast has been studied by means of simulation in a group of works conducted by ElBatt *et al.* [8] and Torrent-Moreno *et al.* [9][10]. A few common observations that apply to these studies are: (i) Either periodic or warning messages are addressed, but not both; (ii) In spite of performance evaluation under various traffic densities, they do not address the impacts of non-uniform and heterogeneous traffic densities attributed to urban traffic systems; (iii) Per-packet delay is in the order of a few milliseconds, which is satisfactory for most safety applications. ElBatt *et al.* [8] suggested a reliability metric termed *packet inter-reception time*, defined as the elapsed time between two consecutive successfully received packets by a vehicle. The authors conducted extensive simulations to measure successful packet delivery and packet inter-reception times under high and low traffic densities in a 2-direction highway scenario with 4 lanes in each direction. In this paper, we adopt the reliability metrics proposed in [8], develop a general analytical framework for their calculation and apply it in the context of an urban scenario. In [9], Torrent-Moreno *et al.* addressed the failure of transmission coordination associated with the IEEE802.11 Distributed Coordination function (DCF) and argued that the level of coordination failure is intensified by the hidden terminal effect. We take into account the fact that the hidden terminal effect is in turn influenced by traffic density and distribution, and study the impact of hidden terminals on safety message reliability under a road network's heterogeneous traffic distribution. Torrent-Moreno *et al.* [10] studied the effects of broadcast storm on the channel. To alleviate the effects, they proposed an adaptive mechanism using transmission power adjustment and tuning of beacon transmission intervals. Yousefi *et al.* [11] studied the delivery ratio and delay of beacon messages with varying packet transmission intervals and packet sizes. Their simulation methodology considered 1-hop broadcast in a stationary large highway scenario and fixed transmission range. According to their simulation results, packet delay was in the order of a few milliseconds, which generally does not constitute a bottleneck for safety applications. They also showed that the packet reception rate decreases significantly when increasing the distance of the receiver from the transmitter, a phenomenon previously observed in [8].

Beyond the simulation studies mentioned above that are specific to vehicular environments, many analytical models have been proposed in the literature to address the performance and reliability of IEEE 802.11 DCF. For the most part, the proposed approaches are variations of the Markov-based performance evaluation method presented by Bianchi [12] and Cali *et al.* [13]; for instance, the implications of an error prone channel was modeled in [14], while retransmission retries and seizing phenomenon were taken into account in [15] and [16], respectively. This framework was extended to IEEE 802.11e QoS differentiation by Engelstad *et al*. [17], who also investigated the channel and application layer performance metrics with respect to non-saturation traffic. In [18], Lyakhov *et al*. studied the performance of IEEE 802.11 networks operating in broadcast mode. They assumed Poisson packet arrival and applied Markov chains to analytically express the mean notification time of broadcast packets. Ma *et al*. [19] studied saturation throughput, delay, and packet delivery rate while taking into consideration the impact of backoff counter freezing in a scenario termed Continuous Freeze Process (CFP). Apart from the above investigative works, efforts have also been made to enhance IEEE 802.11 MAC with respect to the specific requirements of VANETs applications. Recently, Bononi *et al*. [29] proposed an improvement to IEEE 802.11 MAC to support reliable and fast multi-hop broadcast using a dynamic virtual backbone infra-structure.

Most relevant to our work in this paper are studies performed on safety message broadcast within the DSRC framework. Ma *et al*. studied different aspects of safety message broadcast in a series of works. They investigated saturation throughput and packet delivery ratio in [20] and saturation delay in [21]. In a recent work [22], *Ma et al.* analyzed the broadcast performance of safety messages. They considered the impacts of an error-prone realistic channel, hidden terminals, and mobility issues in deriving performance metrics. In their analytical models, they assumed a 1-D highway scenario with vehicles placed on the road according to a Poisson point process with a predetermined density. In [23], Vinel *et al.* modeled IEEE 802.11p VANET as a D/M/1 queuing system and roughly estimated the mean beacon transmission delay and the beacon reception probability. Vinel *et al.* also studied the successful beacon reception probability in [24] and [25] under saturated and unsaturated beacon rates. The common features of the above works are: (i) Beacon messages are treated as random arrivals, and fail to incorporate the periodic nature of beacon messages and consequently fail to characterize the distribution of

the message IRT; (ii) A homogeneous and uniform traffic density is assumed, which is not applicable to urban scenarios.

Our work differs from the above mentioned works in several ways: (i) Instead of solely adopting a simulation approach, we develop an analytical model to generalize the analysis of safety messages' reliability; (ii) We take into consideration the mutual impact of both types of safety messages, i.e. event-driven and periodic; (iii) We study the reliability of safety massage dissemination in an urban traffic scenario, involving road segments connected to a signalized junction, and using a corresponding heterogeneous density model developed in our earlier work [26].

3. Reliability of Safety Message Broadcast

3.1 Assumptions

We make the following assumptions when addressing IEEE 802.11p one hop broadcast communications: (i) the ready-to-send and clear-to-send (RTS/CTS) exchange is disabled, and (ii) ACKs are not transmitted after successful reception. Consequently, no retransmissions are performed and the backoff window size is not adjusted based on the existing load on the channel. Moreover, according to the DSRC standard, it is mandatory that vehicles transmit periodic beacons and event-driven emergency messages on the same channel (channel 178) [1]. Thus, a message can potentially collide with a message of its own type or another type if they are transmitted simultaneously by more than one vehicle.

We assume that the backoff window of event-driven messages W_e is smaller than that of the periodic beacon messages W_b. This is in agreement with IEEE 802.11p standard and implies that event-driven messages are of higher priority than periodic beacons. Additionally, we assume that nodes experience a non-saturated arrival of event-driven messages as a Poisson arrival process with rate λ. Beacon messages, on the other hand, arrive on a periodic basis with inter-arrival time of α time slots. Arrival of a new beacon message cancels out old beacons, since a new beacon is assumed to always contain the most updated vehicle state. As a result, the impact of queuing delay on beacon messages is eliminated.

3.2 Analytical Model

To study the reliability metrics mentioned above, we need to calculate the probability of a vehicle's transmission attempt in a generic time slot. To that end, we propose a Markov-chain model for the backoff process corresponding to a combination of periodic beacons and event-driven messages.

We thus extend the Markov chain model proposed in [22] to account for the periodic nature of beacon transmissions. The chain, shown in Figure 1, consists of a combination of deterministic post backoff (upper stage) and stochastic backoff processes (lower stage). Whenever a vehicle completes its current

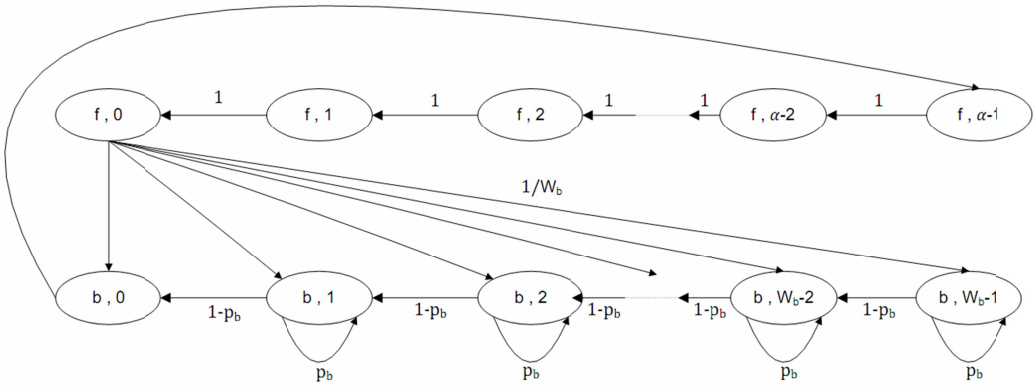

Figure 1. Markov chain model of backoff process for periodic beaconing safety messages

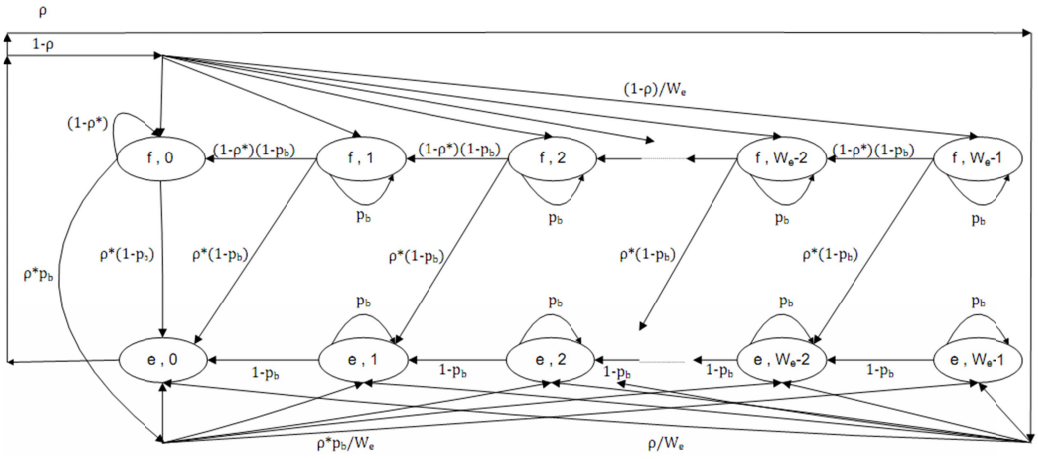

Figure 2. Markov chain model of backoff process for event-driven safety messages

channel contention and transmission attempt, it enters the post backoff stage of length equal to beaconing period $\alpha = \frac{I_b}{\sigma}$, where I_b and σ are the beacon period and time slot duration, respectively. With probability $\frac{1}{W_b}$, a backoff state $(b\,,k)$ is selected and channel contention starts. The probability of a transmission attempt is equivalent to the probability that the backoff process enters state $(b\,,0)$.

To this end we solve the Markov chain shown in Figure 1 to calculate the probability that a vehicle transmits a beacon in a generic time slot, denoted by τ^b. It is easy to verify that the chain steady-state transition and normalization conditions result in:

$$s_{b,k} = \frac{W_b - k}{W_b} s_{b\,,0} \qquad k \in (0\,, W_b - 1) \tag{1}$$

$$s_{f,k} = s_{b\,,0} \qquad k \in (0\,, W_b - 1) \tag{2}$$

$$\sum_{k=0}^{w_r - 1} s_{b\,,k} + \sum_{k=0}^{w_r - 1} s_{f\,,k} = 1 \tag{3}$$

and solving for $s_{b\,,0}$ (equivalent to the probability of transmission attempt τ^b), we obtain:

$$\tau^b = s_{b\,,0} = \frac{2}{W_b + 1 + 2\alpha} \tag{4}$$

The Markov chain corresponding to the backoff process of event-driven messages is shown in Figure 2. This is a simplified model of Engelstad *et al*. [17], customized for broadcast transmission mode. Here, $(f\,,k)$ are post backoff states during which the queue is empty and the node has to wait for a new message to arrive. $(e\,,k)$ represent backoff states where there exists a message for transmission. In this case, with probability ρ, the backoff process is immediately invoked by entering one of the backoff states $(e\,,k)$ chosen randomly. With probability $1-\rho$ the node enters a post backoff stage. While being in a state $(f\,,k)$, if a new message arrives with probability ρ^* (different from ρ) and the channel is sensed idle, the contention process is immediately triggered by directly entering the state $(e\,,k-1)$ in the backoff stage. If the channel is sensed busy, the countdown process is blocked, otherwise a transition to state $(f\,,k-1)$ takes place.

Applying steady-state conditions recursively through the chain, it is easy to show that:

$$s_{f\,,k} = \frac{1-\rho}{W_e} \cdot \frac{1-(1-\rho^*)^{W_e - k}}{1 - p_b} \cdot \frac{s_{e\,,0}}{\rho^*} \qquad k \in (1\,, W_e - 1) \tag{5}$$

$$s_{f\,,0} = \frac{1-\rho}{W_e} \cdot \frac{1-(1-\rho^*)^{W_e}}{(\rho^*)^2} \cdot s_{e\,,0} \tag{6}$$

$$s_{e\,,k} = \frac{(W_e - k)}{W_e \cdot (1-p_b)} \cdot s_{e\,,0} + \frac{(W_e - k) \cdot \rho^* \cdot p_b}{W_e \cdot (1-p_b)} \cdot s_{f\,,k} - s_{f\,,k} \tag{7}$$

and the normalization condition implies

$$\sum_{k=0}^{W_e - 1} (s_{e\,,k} + s_{f\,,k}) = 1. \tag{8}$$

Using (5)-(8), $b_{e\,,0}$ and thus the probability of event-driven message transmission τ^e in a generic time slot we obtain:

$$\frac{1}{\tau^e} = 1 + \frac{W_e - 1}{4(1-p_b)} + \frac{p_b}{(1-p_b)^2} \cdot \frac{1-\rho}{W_e^{\,2}} \cdot \frac{\rho^{*2} W_e (W_e - 1) + (1-\rho^*)^{W_e} (2\rho^* W_e - 2\rho^* + 2) + 2(\rho^* - 1)}{\rho^{*2}} + \frac{1-\rho}{W_e} \cdot \frac{1-(1-\rho^*)^{W_e}}{\rho^{*2}} \tag{9}$$

3.2.1 *Probability of busy channel (p_b)*

The probability of sensing a channel busy event is equivalent to the probability that at least one vehicle is transmitting a message, either a beacon or an event-driven message. This probability can be expressed as:

$$p_b = 1 - \left((1-\tau^b) \cdot (1-\tau^e)\right)^{N_r} \tag{10}$$

where τ^b and τ^e are the probabilities of transmission attempts corresponding to beacon and event-driven messages, described by (4) and (9), respectively. N_r is the number of vehicles in the transmission range (R) of the vehicle under investigation. For uniform traffic distribution (highway scenario) with density β, $N_r = 2\beta R$. For non-uniform traffic distribution (urban scenario), we later give an expression for calculating N_r using the density functions proposed in section 4.

3.2.2 *Probability of successful transmission (p_s)*

Without loss of generality, we address the probability of successful transmission separately for beacon and event driven messages while the mutual impacts are taken into consideration. Denote by p_s^b and p_s^e, the probability of successful transmission of beacon and event-driven messages, respectively. To obtain these probabilities, we account for simultaneous transmissions in the transmission range of a vehicle and transmission(s) from hidden nodes within the hidden area of the sender vehicle. Intuitively, p_s^b and p_s^e are equivalent to the probabilities that exactly one node attempts transmission and no hidden node transmits a message which overlaps in time with the transmission performed by the sender vehicle. Consequently:

$$p_s^b = \tau^b \cdot (1 - \tau^b - \tau^e)^{N_r - 1 + \widetilde{N}_h \frac{T_h^b}{p_b T_s^b + (1-p_b)\sigma}} \tag{11}$$

$$p_s^e = \tau^e . (1 - \tau^b - \tau^e)^{N_r - 1 + \widetilde{N}_h . \frac{T_h^e}{p_b T_s^e + (1-p_b)\sigma}} \tag{12}$$

In (11) and (12), $\widetilde{N}_h$ is the average per vehicle hidden terminal effect on vehicles within the transmission range of a sender vehicle. For uniform traffic distribution with density β, $\widetilde{N}_h = \beta R$. For non-uniform traffic distribution, the hidden terminal nodes fall within the ranges $(x_v - 2R\,, x_v - R)$ and $(x_v + R\,, x_v + 2R)$ on the left and right side of a candidate sender vehicle positioned at x_v; we describe the calculation of $\widetilde{N}_h$ in greater detail in section 4.

T_h in (11) and (12) is the period during which a transmission from a vehicle may overlap with the transmission from a hidden node; hence, $T_h^r = 2T_s^b$ and $T_h^e = 2T_s^e$, where T_s^b and T_s^e are packet transmission time corresponding to beacon and event-driven messages, respectively. The subscript s in T_s^b and T_s^e is introduced to distinguish between duration of a successful message transmission and duration of a message collision. The ratios $\frac{T_h^b}{p_b T_s^b + (1-p_b)\sigma}$ and $\frac{T_h^e}{p_b T_s^e + (1-p_b)\sigma}$ in (11) and (12) are introduced due to the fact that if a node in the hidden area of the sender vehicle starts transmission, the channel will be sensed busy by the remaining vehicles in the hidden area who thus remain silent.

3.2.3 *Calculating ρ^* and ρ*

In the proposed Markov model for event-driven messages, ρ^* is the conditional probability for a new event-driven message to arrive in the queue within a generic slot time, given that at the beginning of the slot the queue was empty. Note that a generic slot can have different lengths due to blocking of the backoff process due to the channel being busy. If the channel is idle (with probability $1 - p_b$), the slot length is σ (nominal slot duration). If a successful beacon or event-driven message transmission occurs on the channel with probability P_s^b and P_s^e, the corresponding

generic slot time will be of length T_s^b and T_s^e, respectively. Otherwise, with probability $p_b - P_s^b - P_s^e$, the slot duration is T_c (collision duration). Therefore, for a Poisson arrival process with rate λ, ρ^* can be expressed as:

$$\rho^* = 1 - \Big((1-p_b)\cdot e^{-\lambda.\sigma} + P_s^b \cdot e^{-\lambda\cdot T_s^b} + P_s^e \cdot e^{-\lambda\cdot T_s^e} + (p_b - P_s^b - P_s^e)\cdot e^{-\lambda T_c}\Big) \quad (13)$$

Note that P_s^b and P_s^e are different from p_s^b and p_s^e described by (11) and (12). More specifically, P_s^b (P_s^e) is the probability of the event that a successful beacon (event-driven) message transmission occurs, taking into account all vehicles within the transmission range of a vehicle, but neglecting the impact of hidden vehicles, since the transmitting vehicle does not have any knowledge about its hidden peers. Accordingly, we explicitly eliminate the effect of hidden terminals as follows:

$$P_s^b = \frac{N_r p_s^b}{(1-\tau^b-\tau^e)^{\bar{N}_h \frac{T_h^b}{p_b T_s^b + (1-p_b)\sigma}}} \quad (14)$$

$$P_s^e = \frac{N_r p_s^e}{(1-\tau^b-\tau^e)^{\bar{N}_h \frac{T_h^e}{p_b T_s^e + (1-p_b)\sigma}}} \quad (15)$$

To calculate ρ, we need to determine the channel service time, which is the time it takes a head-of-line message to access the channel and complete its transmission (whether successfully or not). To that end, we follow the approach proposed in [17] to derive the Z-transform of the Markov chain in Figure 2:

$$\mathrm{D(z)} = \frac{z^{\frac{(P^e+H^e)}{\sigma\cdot R_d}}}{W_e} \cdot \sum_{k=0}^{k=W_e-1} H_{state}^k(z) = \frac{z^{\frac{(P^e+H^e)}{\sigma\cdot R_d}}}{W_e} \cdot \frac{1-(H_{state}(z))^{W_e}}{1-H_{state}(z)} \quad (16)$$

where $H_{state}(z)$ is the Z-transform of each state, expressed as:

$$H_{state}(z) = (1-p_b)\cdot z + P_s^b \cdot z^{\frac{T_s^b}{\sigma}} + P_s^e \cdot z^{\frac{T_s^e}{\sigma}} + (p_b - P_s^b - P_s^e)\cdot z^{\frac{T_c}{\sigma}} \quad (17)$$

The average service time of an event-driven message can be obtained by calculating the derivative of (16) in $z = 1$ (denoted by $D'(1)$ and measured in number of slots). Correspondingly, ρ is obtained as:

$$\rho = 1 - \exp(-\lambda \cdot D'(1)\cdot\sigma) \quad (18)$$

Expressions (9), (10), (11), (12), (13), and (18) are viewed as a system of equations to be solved numerically in order to obtain the values of τ^e , p_b , p_s^b , p_s^e, ρ^* and ρ.

3.2.4 Distribution of IRT

Define $p_I(\gamma)$ to be the complementary cumulative probability of the inter-reception time of beacon messages, namely, the probability that the inter-reception time I of messages from a specific sender is greater than γ. This is equivalent to the probability of at least $\left\lfloor \frac{\gamma}{I_b} \right\rfloor$ consecutive messages (where I_b is the beacon interval) to end in failure, i.e.:

$$p_I(\gamma) = \sum_{I=\gamma}^{\infty}(1-p_s^b)^{\left\lfloor \frac{I}{I_b} \right\rfloor} = \frac{(1-p_s^b)^{\frac{\gamma}{I_b}}}{1-(1-p_s^b)^{\frac{1}{I_b}}} \quad (19)$$

It is also informative to calculate the probability of an event that at least one beacon is received by a vehicle from a sender within a duration γ. Denote by $p_n(\gamma)$ the probability of such an event. We obtain:

$$p_n(\gamma) = \sum_{n=1}^{\left\lfloor \frac{\gamma}{T_b} \right\rfloor}(1-p_s^b)^{\left\lfloor \frac{\gamma}{T_b} \right\rfloor - n}.(p_s^b)^n = \frac{p_s^b\left((1-p_s^b)^{\left\lfloor \frac{\gamma}{T_b} \right\rfloor} - (p_s^b)^{\left\lfloor \frac{\gamma}{T_b} \right\rfloor}\right)}{1-2p_s^b} \quad (20)$$

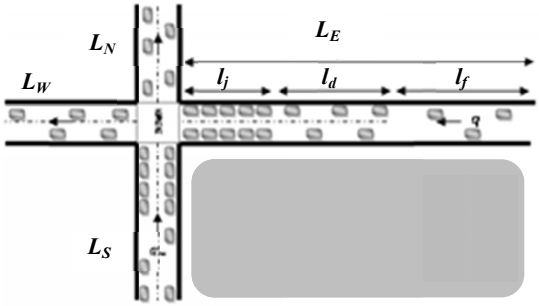

Figure 3. Urban traffic scenario

4. Urban Traffic Model

Our work in this paper is focused on urban traffic systems. In the following, we describe the essential features of a traffic density model for a signalized junction and the road segments linked to it, which is a basic building block of urban traffic (see Figure 3); we refer the interested reader to [26] for further details.

Relevant to our work in this paper is the traffic mobility on the main road segment denoted by L_E in Figure 3. To characterize the dynamics of traffic mobility on the road segment under consideration, we conducted traffic simulations in Paramics [27]. Our observations of traffic density behavior shows that during a red traffic light phase, three regions with different traffic densities coexist along the road segment: 1) a jam traffic density (l_j) caused by vehicles building up a queue, 2) a growing traffic density (l_d) caused by vehicles decelerating as they approach a queue ahead, and 3) an almost constant light traffic density (l_f) caused by vehicles driving in free/stable flow traffic state. During the green phase, a fourth region associated with a different traffic density emerges as vehicles in front of the previously formed queue gradually discharge the queue. By analogy, we identified that the shape and dynamics of the three density regions formed during a red phase and partly during a green phase are analogous to those of a logistic curve [28]. Correspondingly, we proposed two logistic functions to describe traffic density on the road segment under consideration and during a traffic light cycle comprising a red phase followed by a green phase. Assuming the junction is located at position $x = 0$ and t_{red} is the duration of the red phase, the traffic density functions are expressed as:

$$K(x,t) = \begin{cases} A + \frac{K_j - A}{1+exp(B(x-M))} \\ where: \\ A = \frac{l}{HD}\,,\ K_j = \frac{l}{l_{hj}}\,, \\ M = q\cdot t\cdot l_{hj} + {d_b}/{2} \\ B = \frac{2R_d}{V^2}\left(ln\left(\frac{K_j-K_1}{K_1-A}\right) - ln\left(\frac{K_j-K_2}{K_2-A}\right)\right) \end{cases} \quad (21)$$

$$K(x,t) = \begin{cases} max\left(A\,, A + \frac{K_j-A}{1+exp(B(x-M))} - D_{rate}\right)\ s.t\ x < \frac{l_{hj}\cdot(t-t_{red})}{t_r} \\ A + \frac{K_j-A}{1+exp(B(x-M))} \qquad o.w \end{cases} \quad (22)$$

where $K(x,t)$ is the traffic density at position x on the road segment at time instant t, during a red phase (21) or green phase

(22). A is the lower bound traffic density associated with stable/free flow traffic state; K_j is the upper bound traffic density associated with jam traffic density (if $A = 0$ then K_j is called the carrying capacity); B is the growth rate of traffic density from lower bound (A) to upper bound (K_j); M is the reflection point of the logistic curve; l_{hj} is the average jam headway distance which is a known parameter; q is traffic arrival in *vehicles/hour*. V is the speed limit of the road segment; R_d is average deceleration of a vehicle; $d_b = \frac{V^2}{2R_d}$ is the distance it takes for a vehicle with average deceleration and velocity V to fully stop; K_1 and K_2 denote the traffic densities corresponding to the start and end position of the braking distance; l is the number of lanes in a multi-lane road segment; D_{rate} in (22) is the queue discharge rate and is described as:

$$D_{rate} = \begin{cases} \dfrac{l \cdot a \cdot (t' - \frac{x}{l_{hj}} t_r) \cdot t_r}{l_{hj}\left(l_{hj} + a \cdot (t' - \frac{x}{l_{hj}} t_r) \cdot t_r\right)} & s.t\ \ x < \dfrac{l_{hj} \cdot t'}{t_r} \\ 0 & o.w \end{cases}$$

where a is the average acceleration of a vehicle and t' is the relative time instant with respect to the start of the green phase.

4.1 Number of Nodes in Transmission Range (N_r) and Average Number of Hidden Nodes ($\widetilde{N}_h$)

The number of vehicles within the transmission range of a vehicle at position x_v at time instant t is determined by calculating the integral over the density function $K(x,t)$ described by (21) and (22), corresponding to red and green phases of the traffic light cycle:

$$N_r = \int_{\max\,(L_{min}, x_v - R)}^{\min\,(L_{max}, x_v + R)} K(x,t) \cdot dx \tag{23}$$

where L_{min} and L_{max} are the coordinates of the start and end positions of the road segment under consideration, and x_v is the position of the vehicle.

To determine $\widetilde{\mathrm{N}}_{\mathrm{h}}$, we consider the fact that due to the non-uniform traffic distribution, the average per-vehicle number of hidden nodes affecting packet reception is no longer simply half the total number of hidden nodes in the hidden terminal region, as it is in the uniform case. To that end, focusing on the transmission range of the sender vehicle, denote by x_m^r the median position such that half of the total number of vehicles to the right of the sender within its transmission range is located to each side of x_m^r; similarly, define x_m^l to be the median point of vehicles to the left of the sender. In other words, if x_v is the position of the sender vehicle, then, x_m is the point on the road segment that minimizes the following objective function:

$$x_m^{(r,l)} = \mathrm{argmin}_x \left(\frac{N_x}{N} - \frac{1}{2}\right) \quad s.t\ |x - x_v| \le R \tag{24}$$

where $N_x = \int_{x_v}^{\min\,(L_{max}, x_v + x)} K(x,t) \cdot dx$ and $N = \int_{x_v}^{\min\,(L_{max}, x_v + R)} K(x,t) \cdot dx$ are used for calculating x_m^r, while $N_x = \int_{\max\,(\mathrm{L_{min}}, \mathrm{x_v} - \mathrm{x})}^{\mathrm{x_v}} K(x,t) \cdot dx$ and $N = \int_{\max\,(L_{min}, x_v - R)}^{x_v} K(x,t) \cdot dx$ are used for the calculation of x_m^l.

To calculate $x_m^{(r,l)}$ described by (24), we propose a simple algorithm as follows.

Algorithm 1: median position to the right (left) of a sender

Input: $K(x,t)$, x_v, L_{min}, L_{max}, R

Initialize: assign a small positive value (≤ 1) to Δx

$x_m^r \leftarrow x_v$ $(x_m^l \leftarrow x_v)$

$N_{right} \leftarrow \int_{x_v}^{\min\,(L_{max}, x_v + R)} K(x,t) \cdot dx$

$\left(N_{left} \leftarrow \int_{\max\,(L_{min}, x_v - R)}^{x_v} K(x,t) \cdot dx\right)$

1: loop

2: $x_m^r \leftarrow x_m^r + \Delta x$ $(x_m^l \leftarrow x_m^l - \Delta x)$

3: $N_{x_m^r} \leftarrow \int_{x_v}^{\min\,(L_{max}, x_v + x_m^r)} K(x,t) \cdot dx$,

$\left(N_{x_m^l} \leftarrow \int_{\max\,(\mathrm{L_{min}}, \mathrm{x_v} - x_m^l)}^{\mathrm{x_v}} K(x,t) \cdot dx\right)$

4: until $\left|\frac{N_{x_m^r}}{N_{right}} - \frac{1}{2}\right| \le \varepsilon$ $\left(\left|\frac{N_{x_m^l}}{N_{left}} - \frac{1}{2}\right| \le \varepsilon\right)$

5: return x_m^r (x_m^l)

ε in Algorithm 1 is a very small number and the expressions in parentheses correspond to x_m^l.

Correspondingly, the average per-vehicle number of hidden nodes in the right and left direction of the sender is determined as:

$$\widetilde{\mathrm{N}}_h^r = \int_{\min\,(L_{max}, x_v + R + x_m^r)}^{\min\,(L_{max}, x_v + R + x_m^r)} K(x,t) dx \tag{25}$$

$$\widetilde{\mathrm{N}}_{\mathrm{h}}^{\mathrm{l}} = \int_{\max(\mathrm{L_{min}}, \mathrm{x_v} - \mathrm{R} - x_m^l)}^{\max(\mathrm{L_{min}}, \mathrm{x_v} - \mathrm{R})} K(x,t) dx \tag{26}$$

where $\widetilde{\mathrm{N}}_h^r$ and $\widetilde{\mathrm{N}}_h^l$ are the average number of hidden terminals in right and left directions of the sender, respectively.

Using $\widetilde{\mathrm{N}}_h^r$ and $\widetilde{\mathrm{N}}_h^l$, the average per vehicle terminal nodes can be expressed as:

$$\widetilde{\mathrm{N}}_{\mathrm{h}} = \beta \widetilde{\mathrm{N}}_h^r + (1 - \beta) \widetilde{\mathrm{N}}_h^l \tag{27}$$

where $0 \le \beta \le 1$ is a weighting factor and can be determined based on the direction relative to the sender the reception probability of safety message broadcast is considered. In a forward collision warning application (FCW), message reception is not important for vehicles driving ahead of a sender vehicle, thus $\beta = 0$. On the other hand, in a lane change assistance application, reception in both direction are equally important and thus $\beta = 0.5$.

5. Numerical Results

We numerically study the reliability model derived in section 3 within two directions. First, the numerical results of the model are derived for an 8-lane highway scenario and are validated using the results of Elbatt *et al.* [8] simulation work. Second, the results of the model are derived for a 3-lane urban scenario illustrated in Figure 3. Traffic and network parameters corresponding to these scenarios are specified in Table 1. Traffic flow associated with the urban scenario is set to a near-saturation level and determined according to the capacity of the junction; as explained in [26], this traffic flow setting corresponds to an ideal signalized junction, and facilitates predictions for under-saturated and over-saturated traffic conditions near a signalized junction.

5.1 Model Validation

As the scenario simulated in [8] only considers periodic beacons, we set the probability of transmission of event-driven messages to zero to align our model with this scenario. In the scenario, the number of vehicles within the transmission range (i.e. N_r) of a candidate sender in high and low density cases are 358 and 38, respectively. The average per-vehicle number of hidden nodes ($\tilde{N}_h$) calculated using (27) are 179 and 18 for high and low densities. As the traffic is uniformly distributed, $\tilde{N}_h$ is simply half the number of vehicles in the entire hidden terminal area of a node. The numerical results corresponding to [8] are shown in Figure 4. According to Figure 4(a), the probability of successful reception in the dense traffic case decreases with increasing distance from the sender. This can be justified by the fact that for nodes farther from the sender, the number of hidden terminals increases, leading to a higher number of collisions. The mean reception probability achieved by the model and simulations are 0.65 and 0.72, respectively, and the mean difference between the model and simulation results is 8% with standard deviation 4%. The results corresponding to the probability of successful reception in the low density case are depicted in Figure 4(b). Due to the light traffic density, the impacts of simultaneous transmissions and hidden terminal nodes are negligible. The mean reception probability achieved by the model and simulations are 0.96 and 0.98, respectively, and the mean difference is 2% with standard deviation 0.9%.

We applied the mean probabilities of successful reception measured by Elbatt *et al.* and calculated by the model to measure the distribution of IRT in high and low density scenarios. Figure 4(c) represents the complementary cumulative probability as a function of the IRT. The results show that in the low density case, a message is almost always received in less than 200ms. On the other hand, in the high density case, this increases to 400ms for some messages. Furthermore, in the low density case, the probability that the inter-reception time for a message to be above 100ms is quite small. This means that the vast majority of messages arrive in time. The mean difference between results achieved by the model and simulations in high and low density scenarios are 1% and 0.02%, respectively. We thus conclude that the proposed model fits very well with the simulation results of Elbatt *et al* [8].

Table 1. Simulation Parameters

Traffic Parameters	Elbatt *et al.* [8] Scenario	High density: 1920 *vehicles/mile* Low density: 208 *vehicles/mile*
	Urban Scenario	Road length =1 k*m*
		Duration of red phase =50 *s*
		Traffic flow =2740 *vehicles/hour*
		Speed limit =20 *m/s*
		Jam traffic headway distance = 6 *m*
	Transmission range *R* =150 *m*	
	Packet length =100 *bytes*	
	Signal bandwidth = 10 *MHz*	
	Channel Data Rate = 6 *Mbit/s*	
DSRC Parameters	Slot time (σ)=13 μs	
	Propagation delay = 1 μs	
	Preamble length = 40 μs	
	Contention window size W_b = 32 Contention window size W_e = 16	
	Arrival rate λ =1 message/s (event-driven msg.)	
	Beacon period (T_b) = 100 ms	

5.2 Urban Scenario Performance

Our results for the urban scenario are shown in Figures 5 and 6. Figure 5(a) shows traffic density in *vehicles/meter* along the road segment during a red phase, and Figure 5(b) depicts the average per-vehicle number of hidden nodes potentially affecting a vehicle on the road segment. Figure 6 depicts the complementary cumulative probability as a function of IRT. Observe that, by increasing the queue length at the junction, the average per vehicle terminal node increases at positions behind the queue. A maximum number of hidden nodes is observed at positions 301-334 with magnitude 37 at time 50 *sec* (end of the red phase). In addition to the magnitude increase with time, the area with high number of hidden nodes also widens and expands to distances farther from the junction. As the queue length grows larger than *R* (transmission range), the average per vehicle terminal nodes also increases in positions close to the junction. This is shown by the rising curve near the junction from time instant 40 *sec* to 50 *sec*.

It follows from Figure 5(c) that the probability of successful transmission of a vehicle is significantly dependent on the average per vehicle number of hidden nodes. Comparing figures 5(b) and 5(c) reveals that in areas with large number of hidden nodes, the probability of successful transmission is low. In positions 301-334 and at time instant 50 *sec*, for instance, the average successful transmission probability is 0.86, which is the lowest among all positions at the same time instant. In addition, we observe that the density of vehicles within the transmission range of a sender has a very small impact on the probability of successful transmission. At time instance 50 *sec*, the highest number of vehicles within transmission range of a sender is 104, which is observed at position 150m. The number of hidden nodes seen at this position is a small number 3. Correspondingly, the probability of successful transmission is 0.95 at this position, which stresses the fact that the hidden terminal effect is the predominant driving factor determining the achievable successful transmission rate.

We continue the numerical study with the distribution of IRT shown in Figure 6. For three IRT values 100ms, 300ms, and 1s, we calculated the probability of inter-reception time using (19) and depicted the results in Figure 6(a), 6(b), and 6(c) respectively. Again, the worst-case IRT probabilities occur at positions 301-334m with average magnitudes 0.13, 0.002, and 1×10^{-9} corresponding to 100ms, 300ms, and 1s, respectively.

Our results above were given for the red phase of a traffic light. During the green phase, in the first few seconds of the phase, the probability of unsuccessful transmission and probability of high inter-reception time are exacerbated due to a slow initial discharge rate of the queue, thus more positions will experience a high average per-vehicle hidden terminal level. Afterwards, with increasing acceleration, the queue discharges faster and the reliability metrics improve.

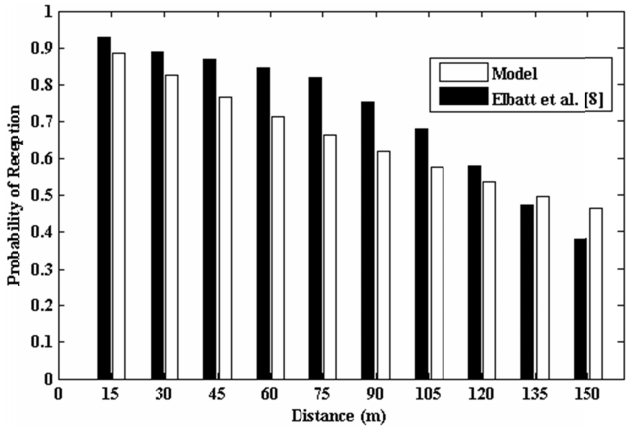

(a)

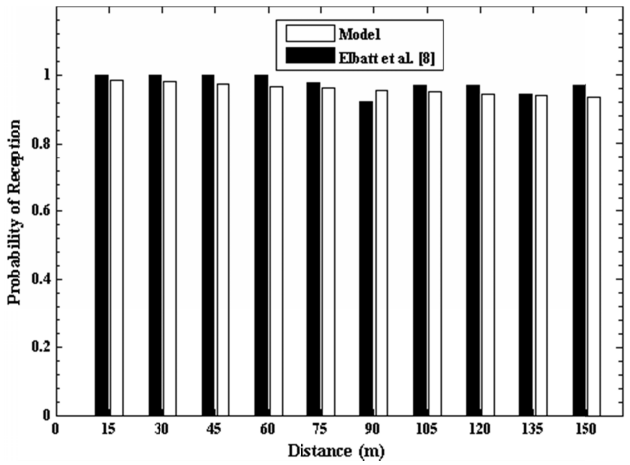

(b)

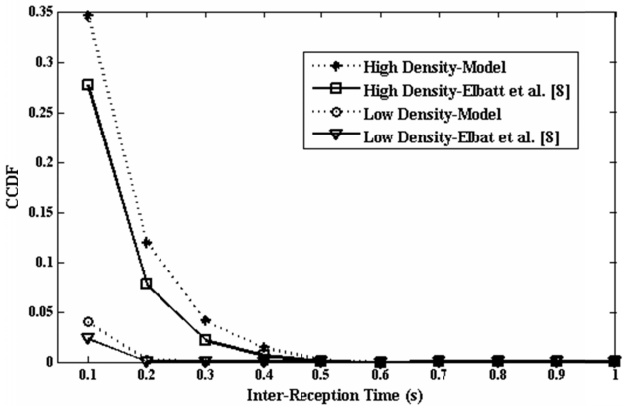

(c)

Figure 4. Comparison of the model and Elbatt *et al.* highway scenario, (a) probability of successful reception in high traffic density, (b)) probability of successful reception in low traffic density, (c) distribution of IRT

5.3 Discussion

The impact of the hidden terminal effect on VANETs has previously been studied in [8][11]. The studies were carried out by simulating free-flow, uniformly distributed vehicular traffic and capturing the packet delivery characteristics. In the validation

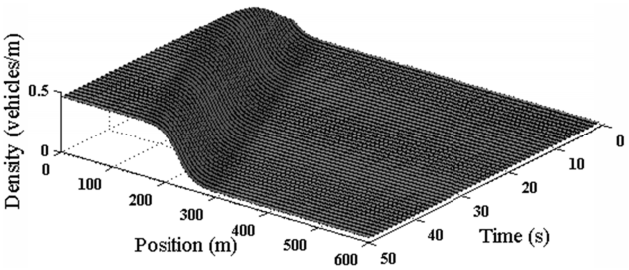

(a)

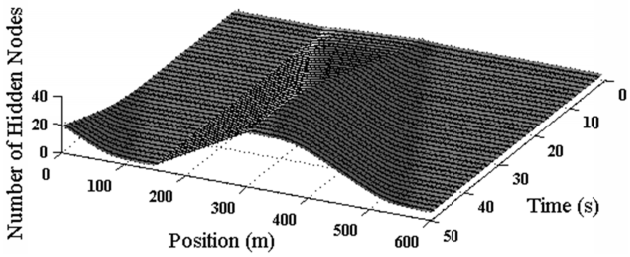

(b)

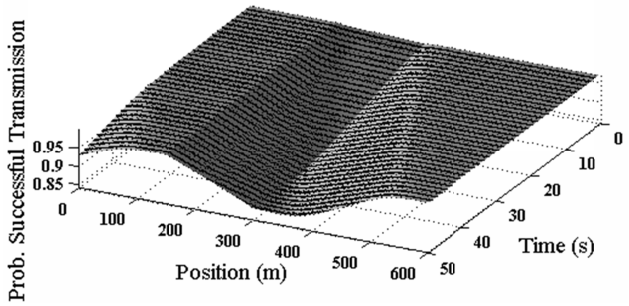

(c)

Figure 5. (a) traffic density, (b) average per vehicle hidden terminal nodes, (c) probability of successful transmission.

of our model in section 5, we verified and corroborated these results. In our study of the reliability performance in the urban scenario, based on a realistic vehicular mobility model around a signalized junction, we find strong evidence that these results can be generalized to cover urban settings as well. One would intuitively suspect that the setting of a signalized junction, characterized by high variations of traffic density, will lead to poor packet delivery performance due to increased overlapping of transmitters. However, our results show that this impact is less significant than the hidden node problem, which is dominant in the urban non-uniform scenario as well. Moreover, we observe that the worst case results take place far from the traffic light queue, where the traffic is either in free-flow or decelerating from high speed. It is notable that, from a traffic safety point of view, these positions are arguably the most important for timely alerting of dangerous traffic conditions, and their lower reliability may correspondingly lead to an increased risk of serious incidents.

Our experiments were carried out at near-saturation traffic conditions, using DSRC communication with moderate (100 byte) payload length. Increasing the traffic load further, or increasing the packet size, will result in lower performance but generally will not change the negative impact dominance of the hidden nodes. It is possible to mitigate the impact of vehicular density by selecting

appropriate radio data rates, but the hidden node problem will still remain a serious issue using the current 802.11p specifications.

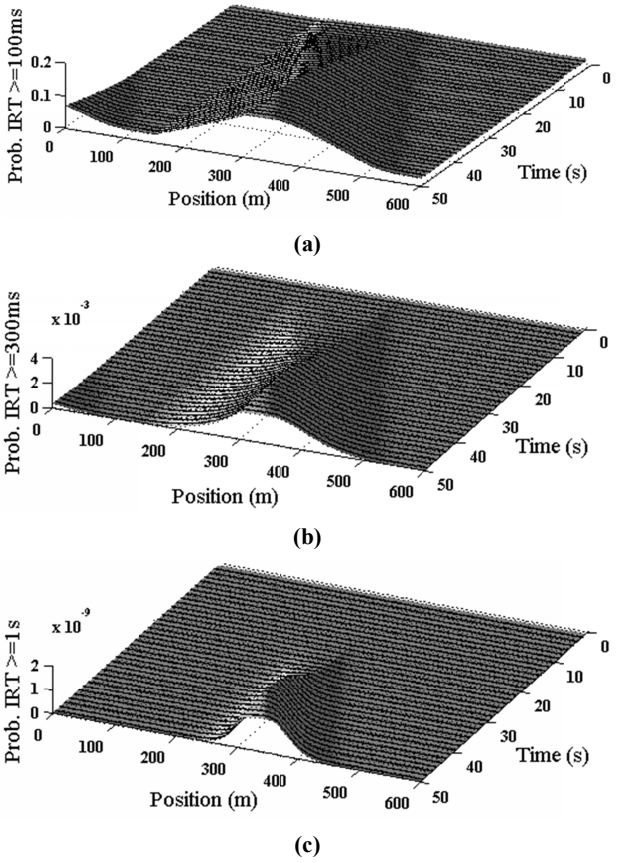

Figure 6. IRT distribution, (a) 100ms, (b) 300ms, (c) 1s

6. Conclusion

Vehicular networks hold great promise in delivering novel road traffic applications that can make road transportation significantly safer than today, limiting risks and catastrophic effects of incidents. It is paramount to these applications that the underlying wireless networks provide stringent packet delivery and delay characteristics. Previous work in this area has focused on investigating the performance of wireless networks in free-flow scenarios, where vehicles are uniformly distributed. This does not hold true in urban settings, where traffic is regulated by signalized junctions. In this paper, we address the urban case by studying the performance of safety messages using a realistic vehicular mobility model which captures the heterogeneous node densities at and around signalized junctions. In line with previous work, we construct Markov models for capturing the delivery probability for event-driven warning messages and the packet inter-reception time for periodic beacons. Combining the Markov models with the urban vehicular density model, for the first time we are able to accurately capture the resulting performance characteristics in a non-uniform density setting. Through a numerical evaluation, we demonstrate that the major impact of the hidden node problem on the reliability performance of safety messages extends to the urban case as well. Importantly, we find that the impact is most significant in the same road sections where the vehicle velocities are highest. These findings call for further work on mechanisms to mitigate the effect of hidden nodes in order to ensure the viability of DSRC-based safety applications.

7. ACKNOWLEDGMENTS

This work was partially sponsored by the Australian Research Council under grant DP0987782.

8. REFERENCES

[1] Standard Specification for Telecommunications and Information Exchange Between Roadside and Vehicle Systems — 5 GHz Band Dedicated Short Range Communications (DSRC) Medium Access Control and Physical Layer Specifications, ASTM E2213 -03, 2010.

[2] IEEE Draft Standard for Information Technology — Telecommunications and information exchange between systems — Local and metropolitan area networks — Specific requirements — Part 11: Wireless LAN Medium Access Control (MAC) and Physical Layer (PHY) specifications, Amendment 6: Wireless Access in Vehicular Environments. IEEE Std 802.11p, July 2010.

[3] K. C. Lee, U. Lee, and M. Gerla. Survey of routing protocols in vehicular ad hoc networks. *Advances in Vehicular Ad-Hoc Networks: Developments and Challenges*, IGI Global, October 2009.

[4] S. Zeadally, R. Hunt, Y.S. Chen, A. Irwin, and A. Hassan. Vehicular ad hoc networks (VANETs): status, results, and challenges. *Telecom Systems*, Springer Netherlands, 2010.

[5] R. Rajaraman. Topology control and routing in ad hoc networks: A survey. *ACM SIGACT News*, 33(2):60-73, 2002.

[6] M. Fiore, J. Harri, F. Filali, and C. Bonnet. Understanding vehicular mobility in network simulation. *IEEE International Conference on Mobile Adhoc and Sensor Systems (MASS)*, Pisa, Italy, October 2007.

[7] J. Harri, F. Filali, and C. Bonnet. Mobility models for vehicular ad hoc networks: A survey and taxonomy. *IEEE Communications Surveys Tutorials*, 11(4):19 –41, 2009.

[8] T. ElBatt, S. K. Goel, G. Holland, H. Krishnan, and J. Parikh. Cooperative collision warning using dedicated short range wireless communications. *3rd ACM international workshop on vehicular ad hoc networks (VANET)*, Los Angeles, CA, USA, September 2006.

[9] M. Torrent-Moreno, S. Corroy, F. Schmidt-Eisenlohr, and H. Hartenstein. IEEE 802.11-based one-hop broadcast communications: Understanding transmission success and failure under different radio propagation environments. *9th ACM/IEEE International Symposium on Modeling, Analysis and Simulation of Wireless and Mobile Systems (MSWiM)*, Torremolinos, Spain, October 2006.

[10] M. Torrent-Moreno and J. Mittag. Adjusting transmission power and packet generation rate of periodic status information messages in VANETs. *3rd ACM international workshop on vehicular ad hoc networks (VANET)*, Los Angeles, CA, USA, September 2006.

[11] S. Yousefi, M. Fathy, and A. Benslimane. Performance of beacon safety message dissemination in Vehicular Ad hoc NETworks (VANETs). *Journal of Zhejiang University SCIENCE A*, 2007.

[12] G. Bianchi. Performance analysis of the IEEE 802.11 distributed coordination function. *IEEE Journal on Selected Areas in Communications,* 18(3):535-547, 2000.

[13] F. Cali, M. Conti, and E. Gregory. IEEE 802.11 wireless LAN: Capacity analysis and protocol enhancement. *IEEE INFOCOM*, San Francisco, CA, USA, March-April 1998.

[14] Q. Ni, T. Li, T. Turletti, and Y. Xiao. Saturation throughput analysis of error-prone 802.11 wireless networks. *Wireless Communications and Mobile Computing*, 5(8):945-956, 2005.

[15] P. Chatzimisios, V. Vitsas, and A.C. Boucouvalas. Throughput and delay analysis of IEEE 802.11 protocol. *5th IEEE international workshop on networked appliances* (IWNA), Liverpool, UK, October 2002.

[16] V.M. Vishnevsky and A.I. Lyakhov. IEEE 802.11 wireless LAN: Saturation throughput analysis with seizing effect consideration. *Cluster Computing*, 5(2):133-144, 2002.

[17] P.E. Engelstad and O.N. Osterbo. The delay distribution of IEEE 802.11e EDCA and 802.11 DCF. *International Performance, Computing, and Communications Conference (IPCCC)*, Phoenix, AZ, USA, April 2006.

[18] A. Lyakhov, V. Vishnevsky, and P. Poupyrev. Analytical study of broadcasting in 802.11 ad hoc networks. *2nd International Conference on e-Business and Telecommunication Networks* (ICETE), Reading, UK, October 2005.

[19] X. Ma and X. Chen. Performance analysis of IEEE 802.11 broadcast scheme in ad hoc wireless LANs. *IEEE Transactions on Vehicular Technology,* 57(6):3757-3768, 2008.

[20] X. Ma and X. Chen. Saturation performance of IEEE 802.11 broadcast networks. *IEEE Communications Letters,*11(8):686-688, 2007.

[21] X. Chen, H. Refai, and X. Ma. Saturation performance of IEEE 802.11 broadcast scheme in ad hoc wireless LANs. *IEEE Vehicular Technology Conference* (VTC), Baltimore, MD, USA, September-October 2007.

[22] X. Ma, X. Chen, and H. Refai. Delay and broadcast reception rates of highway safety applications in vehicular ad hoc networks. *IEEE INFOCOM*, *Mobile Networks for Vehicular Environments Workshop*, Anchorage, AK, USA, May 2007.

[23] A. Vinel, V. Vishnevsky, and Y. Koucheryavy. A simple analytical model for the periodic broadcasting in vehicular ad-hoc networks. *4th IEEE Broadband Wireless Access Workshop*, New Orleans, LA, USA, December 2008.

[24] A. Vinel, D. Staehle, and A. Turlikov. Study of beaconing for car-to-car communication in vehicular ad-hoc networks. *IEEE VehiMob Workshop*, Dresden, Germany, June 2009.

[25] A. Vinel, Y. Koucheryavy, S. Andreev, and D. Staehle. Estimation of a successful beacon reception probability in vehicular ad-hoc networks. *International Wireless Communications and Mobile Computing Conference (IWCMC)*, Leipzig, Germany, June 2009.

[26] S. Bastani, B. Landfeldt, and L. Libman. A Traffic Density Model for Radio Overlapping in Urban Vehicular Ad hoc Networks. *IEEE Conference on Local Computer Networks (LCN)*, Bonn, Germany, October 2011.

[27] Quadstone Paramics, 2008. Available at: http://www. paramicsonline.com.

[28] S. E. Kingsland. Modeling nature: episodes in the history of population ecology. *University of Chicago Press*, ISBN 0-226-43728-0.

[29] L. Bononi, M. Di Felice, and S. Pizzi. Dba-MAC: Dynamic Backbone-Assisted Medium Access Control Protocol for Efficient Broadcast in VANETs. *Journal of Interconnection Networks*, 10(4):321-344, 2009.